Supporting Information

A Solution-Processed Ag@ZnO Core-Shell Nanowire Network for Stretchable Transparent Electromagnetic Interference Shielding Application

Siyi Yan[†], *Henan Wang*[‡], *and Peng Li*[*,‡]

[†]School of Information Technology, Jilin Agricultural University, Changchun 130118, P. R. China

[‡]Key Laboratory of UV-Emitting Materials and Technology, Ministry of Education, Northeast Normal University, Changchun 130024, P. R. China

[*]Corresponding author, email address: lip032@nenu.edu.cn

METHODS

Preparation of the Ag NW network. The Ag NW network was fabricated by chemical plating silver on the electrospun polymer NW network templates. Firstly, the electrospun precursor solution consisted of 8 wt% of polyvinyl butyral (PVB, Aladdin) and 10 wt % of anhydrous tin(II) chloride (Sinopharm) in n-butanol (Aladdin). Electrospinning was completed by using a voltage of +8 kV. The resulting PVB/$SnCl_2$ NWs were transferred onto different transparent substrates (glass slide/PDMS). Then, the argon plasma-treated PVB/$SnCl_2$ NWs were immersed into 25 g/L of $AgNO_3$ (99.9995%, Sinopharm) aqueous solution to grow Ag catalytic nano-seed layers for 30 min. Finally, electroless deposition was achieved by using Tollen's reaction. In detail, the glucose ($C_6H_{12}O_6$) and silver nitrate ($AgNO_3$) were added in deionized water at the same concentration

(0.04 M). After the complete dissolution of $C_6H_{12}O_6$, absolute methanol was added in the $C_6H_{12}O_6$ solution ($C_6H_{12}O_6$:CH_3OH = 2:1) to form *reducing agent*. Sodium hydroxide (NaOH, 0.25 M) was added (NaOH:$AgNO_3$ = 1:500) and ammonium hydroxide (NH_4OH, 28–32%) were subsequently added dropwisely until the $AgNO_3$ solution became clear to form *silver solution*. Then the *reducing agent* was mixed with the *silver solution* (1:1) with vigorously stirring. The resulting solution was quickly poured into a plastic petri-dish containing the Ag-seeded PVB NW network on the PDMS substrate. After the Ag reaching a desirable thickness, the sample was rinsed in a solution (H_2O:NH_4OH = 20:1) for 30 s to quench the reaction, and subsequently rinsed in deionized water.

Synthesis of the Ag@ZnO core-shell NW network. The Ag@ZnO core-shell NW network was achieved by an electrodeposition process using a sourcemeter (Keithley 2461B). Ag-paste electrodes were coated on the one end of the Ag NW network on the glass slide, which was placed in a 0.1 M/L $Zn(NO_3)_2$ aqueous solution (99.99%, Sinopharm). The electrolyte was placed on a hot plate which is set to 70 ºC to facilitate the decomposition of $Zn(OH)_2$ into ZnO. The electrodeposition current of 10 to 20 mA was applied across a titanium iridium plating anode and Ag NW network. The thickness of the ZnO shell layer was controlled by adjusting the time of electrodeposition.

Fabrication of the Ag NWs/ZnO composite films. For comparison, the Ag NWs/ZnO films were prepared by magnetron sputtering ZnO film on the Ag NW network using a sputtering system (SYSKEY A100001). The sputtering chamber was evacuated to a base pressure of 5×10^{-7} Torr. A ZnO target was used for depositing ZnO films with work pressure of 5 mTorr and DC power of 80 W. The film thickness was controlled by changing the sputtering time at deposition rate of 3 A s^{-1}. The ZnO was deposited in Ar (99.9%) atmosphere and at room temperature. The substrate holder was rotating during deposition with a speed of 12 r.p.m. For improving the surface

properties of the ZnO film, oxygen plasma treatment was performed on the substrate for 2 min inside the plasma cleaner (Diener, Femto). Bias power (40 W) and pressure (0.5 mbar) were used in O_2 (20 sccm) atmosphere.

Characterization. The surface morphology of the Ag NW network and the Ag@ZnO core-shell NW network was observed by using scanning electron microscopy (SEM, Hitachi S-4800). Electrical characterizations were conducted with a constant current source (Keithley 2461B). The sheet resistance was measured with a four-probe system (RTS-9, 4Probes Tech Ltd. Guangzhou, China). The resistance of the film was calculated by measuring the I–V curve using a Keithley 2461B sourcemeter. A Hitachi UH4150 spectrometer with an integrating sphere was used to measure the transmission spectra of the Ag@ZnO core-shell NW network and Ag NW network. The transmittance results were calibrated against those of a clean glass slide or PDMS substrate. A constant wet and humidity box (YTX-PTLM80, Dongguan Yuantai Co., Ltd) was used in the damp heat test for more than 120 h. A constant current or voltage was applied to the heaters using a Keithley 2461B sourcemeter. The surface temperature of the heater was recorded using an infrared thermometer (RNO IR-160P).

Electromagnetic interference shielding performance measurements of the Ag@ZnO core-shell NW network. First, the samples were prepared on the PDMS substrate. The PDMS is transparent to electromagnetic waves and makes little contribution to the electromagnetic interference (EMI) shielding performance of the Ag NW network and the Ag@ZnO core-shell NW network. The thickness of the tested samples was 1.22 mm. The samples were cut into slightly larger dimension compared to the waveguide window and then mounted between two waveguides, aligned, and tightly fixed to avoid any leakage paths. The EMI shielding performance was measured by a waveguide method using a vector network analyzer (Keysight N5222B PNA) and

at least 20 samples were tested. All the samples are in the same size when tested in the same frequency range. S-parameters (S_{11}, S_{22} for reflection and S_{12}, S_{21} for transmission of the EM wave) and the complex permittivity (ε' and ε'') of the samples were recorded. The total shielding effectiveness (SE_T) is the sum of EMI SE by three mechanisms, shielding effectiveness by reflection (SE_R) and by absorption (SE_A), and multiple internal reflections (SE_{MR}). In particular, the SE_{MR} is almost negligible when the SE_A is larger than 10 dB, where most of the EM waves are reflected back or dissipated as heat inside the material. Thus, SE_T consists of SE_R and SE_A. The total wave reflection coefficient (R) and transmission coefficient(T) can be described as:

$$R=10(S_{11}/10) \quad (1)$$

$$T=10(S_{21}/10) \quad (2)$$

The absorption coefficient (A) can be calculated as: $A = 1 – R − T$. The SE_A and SE_R were then calculated by the equations:

$$SE_A=-10\lg[T/(1-R)] \quad (3)$$

$$SE_R=-10\lg(1-R) \quad (4)$$

And the dielectric dissipation factors and the Cole–Cole semicircle curves were obtained from the complex permittivity. To measure the electromagnetic shielding characteristics of samples after stretching, the samples were stretched and released repeatedly using the experimental setup of mechanical stability test (Mark-10). The samples were then connected to waveguides and measured.

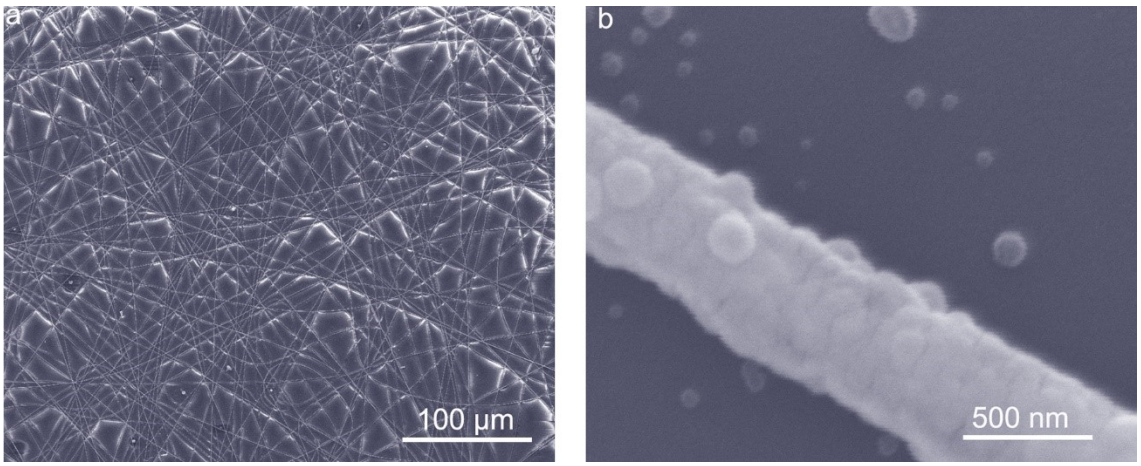

Figure S1. Low- and high- magnification SEM images of the Ag NW network (a) and individual Ag NW (b), respectively. It can be seen that the diameter of the Ag NW is about 550 nm, and the length of the Ag NWs is more than hundreds of micrometers. Therefore, the length-to-diameter ratio of our Ag NWs is higher than 10^3, which ensures the good optoelectronic performance as a transparent electrode by forming sparse networks.

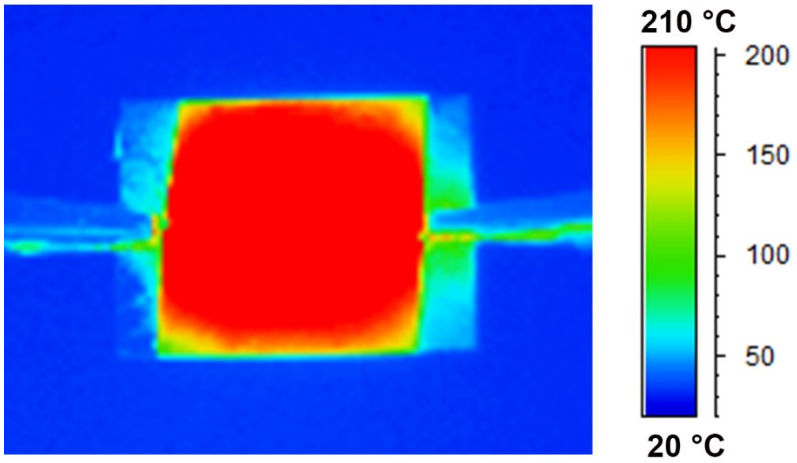

Figure S2. Infrared thermal image of Ag@ZnO core-shell nanowire network transparent heater under applied constant voltage of 8 V.

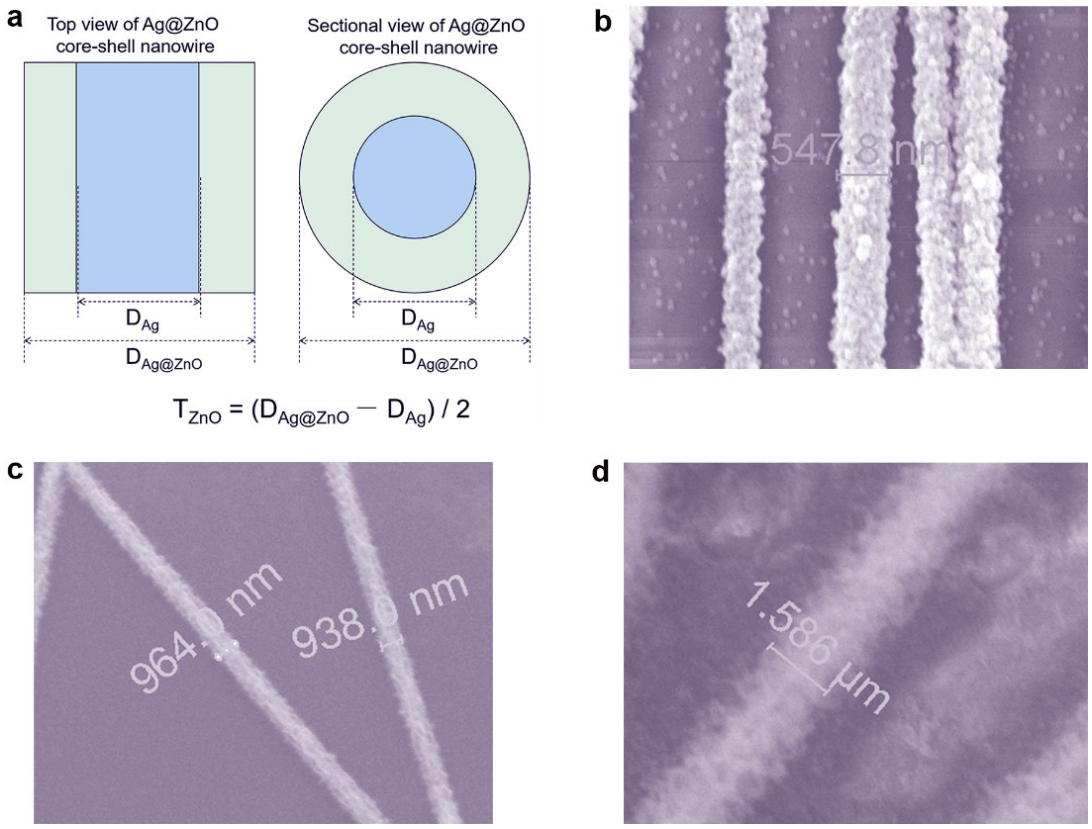

Figure S3. (a). Top viewed and sectional viewed diagrams of the Ag@ZnO core-shell NW illustrating the thickness calculation method of ZnO shell layer (T_{ZnO}) according to the diameter of Ag NWs (D_{Ag}) and Ag@ZnO core shell NWs ($D_{Ag@ZnO}$). (b-d) Typical SEM images of the Ag NWs and the Ag@ZnO core-shell NWs with different ZnO shell layer thicknesses.

Table S1. Comparison of the transmittance at 550 nm and the EMI SE_T of our Ag@ZnO core-shell NW network with other transparent EMI shielding materials reported in literature.

Material and Structure	**Transmittance at 550 nm (%)**	**EMI SE_T (dB) in the X-band**	**Ref.**
Ag NW network	70	30	S51
Ag NW network	73	37	S52
Ag NW network	93	20	S53
Ag NF network	89	20	S54
Ag NW network	91	28	S55
ITO-Au-ITO film	69	26	S57
MXene-CNT film	82	0.8	S58
rGO-Ag NW film	85	24	S59
Graphene-metal mesh	90	14	S60
Cu-Ag NW network	58	55	S61
Fe_3O_4-Ag NW network	90	23	S62
7 μm-thick Ni-Ag mesh	83	43	S64
Ag NW mesh	67	42	S65
Co-doped SnO_2 film	67	20	S66
$Ti_3C_2T_x$ film	75	4	S67
Ag@ZnO core-shell NW network	**88**	**31**	**This work**

Supplementary Reference

1. Hu, M.; Gao, J.; Dong, Y.; Li, K.; Shan, G.; Yang, S.; Li, R. K.-Y. Flexible Transparent PES/Silver Nanowires/PET Sandwich-Structured Film for High-Efficiency Electromagnetic Interference Shielding. *Langmuir* **2012**, *28*, 7101−7106.
2. Jia, L.-C.; Yan, D.-X.; Liu, X.; Ma, R.; Wu, H.-Y.; Li, Z.-M. Highly Efficient and Reliable Transparent Electromagnetic Interference Shielding Film. *ACS Appl. Mater. Interfaces* **2018**, 10, 11941−11949.
3. Jung, J.; Lee, H.; Ha, I.; Cho, H.; Kim, K. K.; Kwon, J.; Won, P.; Hong, S.; Ko, S. H. Highly Stretchable and Transparent Electromagnetic Interference Shielding Film Based on Silver Nanowire Percolation Network for Wearable Electronics Applications. *ACS Appl. Mater. Interfaces* **2017**, *9*, 44609−44616.
4. Lin, S.; Wang, H.; Wu, F.; Wang, Q.; Bai, X.; Zu, D.; Song, J.; Wang, D.; Liu, Z.; Li, Z. Room-Temperature Production of Silver-Nanofiber Film for Large-Area, Transparent and Flexible Surface Electromagnetic Interference Shielding. *NPG Flex. Electron.* **2019**, *3*, 1−8.
5. Yang, H.; Bai, S.; Guo, X.; Wang, H. Robust and Smooth UV-Curable Layer Overcoated AgNW Flexible Transparent Conductor for EMI Shielding and Film Heater. *Appl. Surf. Sci.* **2019**, *483*, 888−894.
6. Erdogan, N.; Erden, F.; Astarlioglu, A. T.; Ozdemir, M.; Ozbay, S.; Aygun, G.; Ozyuzer, L. ITO/Au/ITO Multilayer Thin Films on Transparent Polycarbonate with Enhanced EMI Shielding Properties. *Curr. Appl. Phys.* **2020**, *20*, 489−497.
7. Weng, G. M.; Li, J.; Alhabeb, M.; Karpovich, C.; Wang, H.; Lipton, J.; Maleski, K.; Kong, J.; Shaulsky, E.; Elimelech, M. Layer-by-Layer Assembly of Cross-Functional Semi-Transparent Mxene-Carbon Nanotubes Composite Films for Next-Generation Electromagnetic Interference Shielding. *Adv. Funct. Mater.* **2018**, *28*, 1803360.
8. Kim, D. G.; Choi, J. H.; Choi, D.-K.; Kim, S. W., Highly Bendable and Durable Transparent Electromagnetic Interference Shielding Film Prepared by Wet Sintering of Silver Nanowires. *ACS Appl. Mater. Interfaces* **2018**, *10*, 29730−29740.
9. Han, Y.; Liu, Y.; Han, L.; Lin, J.; Jin, P. High-Performance Hierarchical Graphene/Metal-Mesh Film for Optically Transparent Electromagnetic Interference Shielding. *Carbon* **2017**, *115*, 34−42.

10. Kim, D.-H.; Kim, Y.; Kim, J.-W. Transparent and Flexible Film for Shielding Electromagnetic Interference. *Mater. Design* **2016**, *89*, 703−707.
11. Wang, Z. X.; Jiao, B.; Qing, Y. C.; Nan, H. Y.; Huang, L. Q.; Wei, W.; Peng, Y.; Yuan, F.; Dong, H.; Hou, X.; Wu, Z. X. Flexible and Transparent Ferroferric Oxide-Modified Silver Nanowire Film for Efficient Electromagnetic Interference Shielding. *ACS Appl. Mater. Interfaces* **2020**, *12*, 2826−2834.
12. Shen, S.; Chen, S.-Y.; Zhang, D.-Y.; Liu, Y.-H. High-Performance Composite Ag-Ni Mesh Based Flexible Transparent Conductive Film as Multifunctional Devices. *Opt. Exp.* **2018**, *26*, 27545−27554.
13. Gu, J.; Hu, S.; Ji, H.; Feng, H.; Zhao, W.; Wei, J.; Li, M. Multi-Layer Silver Nanowire/Polyethylene Terephthalate Mesh Structure for Highly Efficient Transparent Electromagnetic Interference Shielding. *Nanotechnology* **2020**, *31*, 185303.
14. Park, J. S.; Lee, S. S.; Park, I. K. Visible and IR Transparent Co-Doped SnO_2 Thin Films with Efficient Electromagnetic Shielding Performance. *J. Alloy. Compd.* **2020**, *815*, 152480.
15. Yun, T.; Kim, H.; Iqbal, A.; Cho, Y. S.; Lee, G. S.; Kim, M. K.; Kim, S. J.; Kim, D.; Gogotsi, Y.; Kim, S. O.; Koo, C. M. Electromagnetic Shielding of Monolayer MXene Assemblies. *Adv. Mater.* **2020**, *30*, 1906769.